International Journal of Robotics and Control Systems
Vol. 4, No. 4, 2024, pp. 2073-2094
ISSN 2775-2658
http://pubs2.ascee.org/index.php/ijrcs

Simulation and Modeling with Designing for the Proportional, Integral and Derivative Control of Industrial Robotic Arm by Using MATLAB/Simulink

Salam Waley Shneen [a,1,*], Hasan H. Juhi [b,2], Hiba Ali Najim [c,3]

[a] Energy and Renewable Energies Technology Centre, University of Technology-Iraq, Baghdad, Iraq
[b] Communication Engineering Department, University of Technology, Baghdad, Iraq
[c] Department of Electromechanical Engineering, University of Technology, Baghdad, Iraq
[1] salam.w.shneen@uotechnology.edu.iq; [2] Hasan.H.Juhi@uotechnology.edu.iq; [3] eme.19.36@grad.uotechnology.edu.iq
* Corresponding Author

ARTICLE INFO

Article history
Received August 21, 2024
Revised October 17, 2024
Accepted November 19, 2024

Keywords
Robotic Arm;
DCM;
PID Controller;
Open Loop System;
Close Loop System;
Transfer Function;
One position at Different Angles;
Multi position at Different Angles

ABSTRACT

This study aims to develop a control system for a robot arm, designed to perform precise movements along a predefined path, suitable for various industrial applications. The robot arm's movements are driven by three electric motors, each responsible for controlling a joint, enabling the arm to follow the required path accurately. To manage the complexity of multiple motors and dynamic movement requirements, an automated control system has been developed, tailored to meet the specific demands of the proposed task. A highly efficient, reliable, and safe control system design is being developed and simulated to evaluate its effectiveness in executing the required path. A simulation model is being constructed to assess the system's ability to follow the prescribed path, its responsiveness to disturbances and transient conditions, and the overall accuracy of the arm's movements. Simulation results will be analyzed to determine the system's performance across various scenarios, evaluating its adaptability to the work environment and its ability to achieve tasks with high accuracy, thereby enhancing system effectiveness.

1. Introduction

Articulated robots have garnered significant attention for their flexibility, versatility, and wide range of motion, thanks to their multiple articulated axes. These characteristics make them invaluable in various industrial, medical, and other applications. In designing and controlling robotic motion, it's essential to transform the motion from the joint kinematic domain to the Cartesian domain. There are two types of motion: Forward kinematics and reverse kinematics. In forward kinematics, the robot is guided toward a desired goal by adjusting the joint angles to achieve smooth and coordinated movement. Inverse kinematics, on the other hand, involves computing the joint configurations necessary to achieve specific workspace coordinates [1]-[3]. This process is crucial for various robotics tasks, including path-following, object manipulation, and precise scene observation. Due to its extreme importance, inverse kinematics has been studied extensively, with many techniques available to solve it quickly and reliably [4]-[6]. Robotic systems are utilized in a wide range of applications, from industrial and agricultural to domestic, military, and healthcare settings. Robotic systems are one of the systems that can be relied upon to perform any suitable function in many

different fields and applications. The robot arm is central to executing most of the tasks assigned to a robotic system, following a predetermined path designed to accomplish specific objectives [7]-[9]. Control systems are critical components that enhance performance and mitigate disturbances in robotic systems. The robot performs most of the tasks that can be done [10]-[12]. Robots alleviate human fatigue, save time and effort, and enhance performance and productivity in industrial settings. Robots can also be employed to perform tasks that are dangerous to humans, such as military applications such as removing mines and rubble in dangerous places as a result of disasters and others [13]-[15]. Robot movement is driven by electric motors, which provide the necessary mechanical power to perform various tasks [16]-[18]. To ensure proper functioning, electric motors require a control unit and sensors that provide feedback, continuously updating system information. Modern control techniques, such as Pulse Width Modulation (PWM), along with traditional Proportional, Integral and Derivative (PID), expert, or intelligent controllers, are employed to optimize motor performance and enhance system efficiency [19]-[21].

The research contribution of this study is to develop a control system for an articulated robotic arm by simulating this arm using MATLAB to perform precise movements based on the PID controller proposed in this research to perform precise movements along a predefined path, suitable for various industrial applications.

2. Modeling of Direct Current Motor (DCM) for Robotic Arm System

The electric motor system can be modeled and represented for various applications including industrial applications such as robotics. The motor simulation model can be constructed by looking at the schematic showing the DC motor (DCM) as shown in Fig. 1 and also by the DCM block diagram shown in Fig. 2. It is usually used because it has many advantages such as fast response, energy efficiency, lower noise, low moment of inertia ratio, small size, high accuracy, low manufacturing cost, high torque when working, fast change of rotation direction, and bearing any instant fixed position in the robotic mechanism [22]. By representing the electrical and mechanical aspects of the motor, the transfer function can be written in the following formula [23]:

$$\frac{\Theta_s}{V_a} = \frac{K_t}{s(L_a s + R_a)(J_m s + B_m) + K_t K_b s} \quad (1)$$

Where the symbols are represented by the following Table 1:

Table 1. Symbols of DCM parameters [24]

Criterion	Symbols
Armature resistance	Ra
Armature inductance	La
Moment of inertia	Jm
Friction coefficient	Bm
Torque constant	KT
Back emf constant	KB

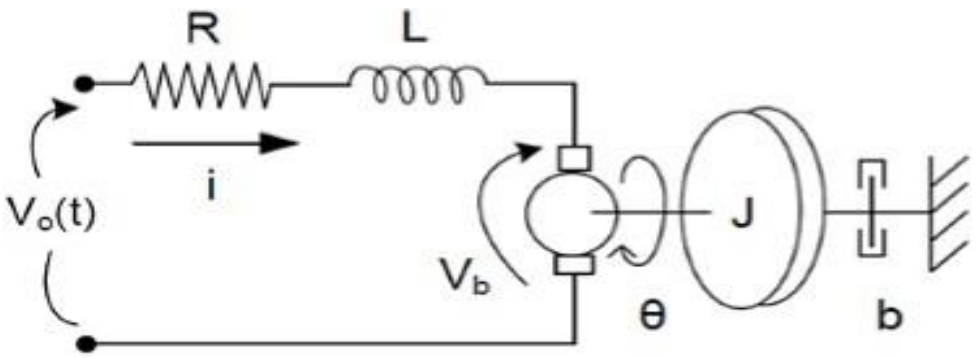

Fig. 1. DCM diagrams

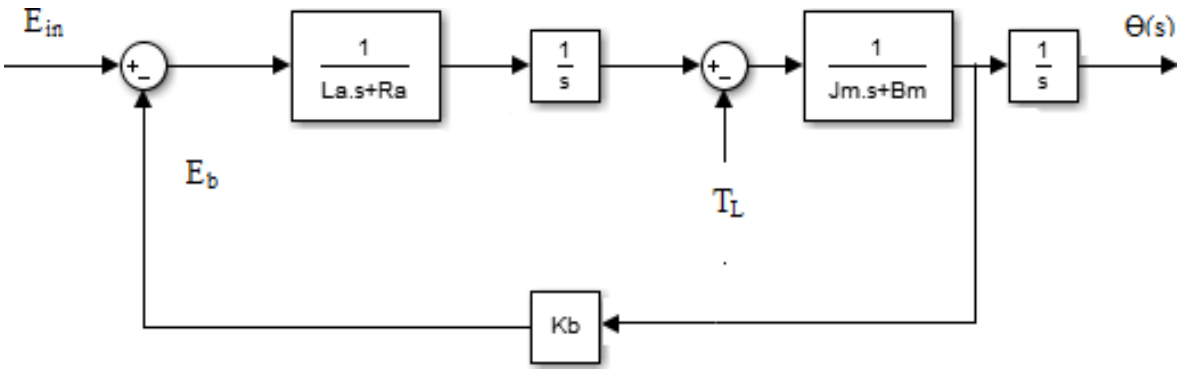

Fig. 2. Representation a DCM block diagram

The equation of transfer function for the system can be represented by [1]:

$$\hat{G}_c(s) = \frac{0.072767z}{z^2 - 1.350753z + 0.423020} \tag{2}$$

$$\hat{G}_c(s) = \frac{0.065985z}{z^2 - 1.350992z + 0.416566} \tag{3}$$

$$\hat{G}_c(s) = \frac{0.059974z}{z^2 - 1.360473z + 0.420346} \tag{4}$$

This study transforms the z-domain into the s-domain because the application of the s-domain concept is ideal for the analysis of systems with transient responses of linear systems that are not affected by time. The output signals appear linear with the input signals. These systems are necessarily dynamic and are mostly subject to second-order differential equations. Almost all real systems encountered by LTIS control systems are modeled to simplify the problem. To facilitate the calculations, the equations developed in this way are solved by a suitable processing program such as MATLAB. Where the new equation in s-domain can be written:

$$Hc = \frac{0.3899\ s + 9.033}{s^2 + 8.667\ s + 0.4203} \tag{5}$$

$$Hc = \frac{0.4719\ \mathrm{s}\ +\ 10.85}{s^2 + 8.393\ \mathrm{s}\ +\ 12.13} \tag{6}$$

$$Hc = \frac{0.39\ \mathrm{s}\ +\ 9.034}{s^2 + 8.667\ \mathrm{s}\ +\ 9.019} \tag{7}$$

The system can be represented mathematically by identifying the components of the system and placing appropriate symbols on them. The system is represented dynamically by determining the angles at which the robot arm moves, and the length of the ulna and the length of the arm are determined, in addition to determining their mass. The symbol (θ) can be used for the angle, and the symbol for the change can be written with the letter (i), so the first component of the system can be written with the symbol (θi). In the same way, the rest of the components can be written to include the mass and the arm, respectively, with the symbols (li and mi).

Mathematical equations are written to represent the system through the behavior expected to perform most natural functions, and include the kinetic energy and moments necessary for the movement of the joints, to include the moment of movement of the arm and its kinetic energy.

The paths can be determined by setting the coordinates and angles of joint movement. For example, the position of the outstretched arm attached to the body is aligned along the negative y-axis, and the angle is considered zero since it is in a state of immobility, as in position One. Another

example of the arm is at shoulder level, extended to the right or left side, i.e. the arms. Therefore, it can be said that the arm is placed at a ninety angle from its previous state attached to the body. The first and second examples represent a model of two paths that were in motion for the entire arm, while there are cases in which the movement and angles of the two joints differ, as in positions Three. And four and five. In the two positions, we notice a ninety-ninth angle between the ulna and the arm, and another angle that is acute, that is, less than ninety, or obtuse, that is, greater than ninety and less than one hundred and eighty [22]-[24]. Example of a position of the arm attached to the body can be considered on the negative y-axis shown in Fig. 3.

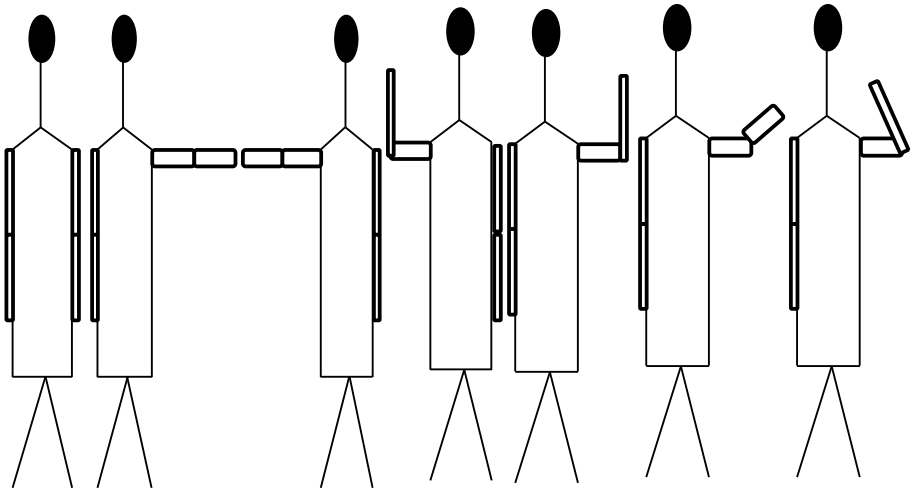

Fig. 3. Example of a position of the arm attached to the body can be considered on the negative y-axis

The mathematical representation of the kinematics can be found simply for two link robot arms through equations (1) and (2), which represent the equations of kinematics for the first and second axes, respectively. This gives the final position of the fingertip along the x- and y-axes.

$$Y = L1sin\theta1 + L2\,si(\theta1 + \theta2) \tag{8}$$

$$X = L1cos\theta1 + L2\,co(\theta1 + \theta2) \tag{9}$$

Where L1 and L2 they represent the length of the link as shown in Fig. 4.

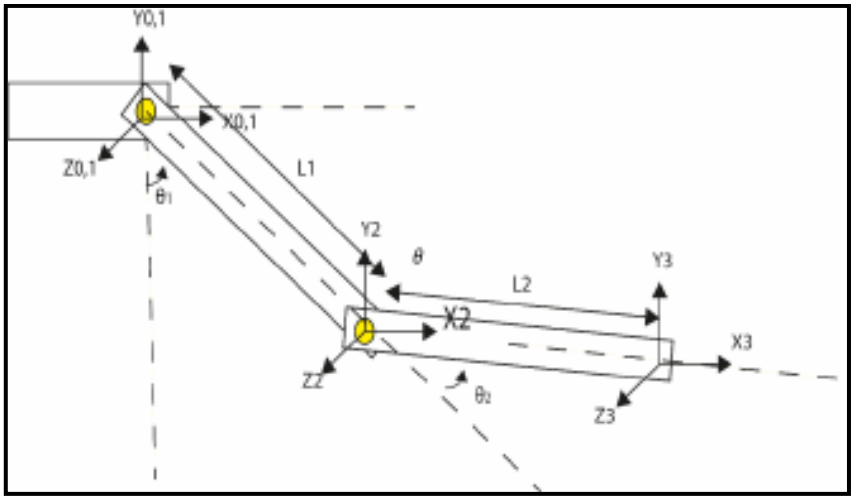

Fig. 4. two link arm robots [25]

The other method, the inverse kinematics, is the most commonly used, as it gives results based on the values of the position inputs. It can be represented mathematically by equations (3) and (4) [25].

$$\theta_1 = \text{atan}\left(\frac{y}{x}\right) + \tan^{-1}\left(\frac{L_2 sin\theta_2}{L_{1+}L_2 cos\theta_2}\right) \quad (10)$$

$$\theta_2 = +\cos^{-1}\left(\frac{x^2 + y^2 - L_1^2 - L_2^2}{2L_1L_2}\right) \quad (11)$$

Many laboratories and production companies rely on robotic systems for some functions, which depend on the movement of the robot arm. To determine the required movement and ensure the appropriate path, this requires working to simulate these systems based on dynamic theory, as well as describing and analyzing the movement system of the robot arm through the correctness and accuracy of its movement path. Simulation can be performed after building the appropriate mathematical model for the robot arm and adopting the laws that control the position of the arm and its appropriate movement. The appropriate design can be developed after conducting tests for the proposed model, achieving the required path with high accuracy, system efficiency, speed of response, overcoming disturbances, stability of the system under different operating conditions, and overcoming transient conditions [26]-[28].

Simulation of any system helps in developing the appropriate design. Simulation requires building a model. Building the model depends on mathematical representation. Any system can be represented mathematically using mathematical relationships that connect its parts. The human arm performs functions through its movement. The visual arm moves with the help of the muscular system of the skeletal system, and the arm can rotate at different angles depending on the function. A model of a robotic arm can be developed to mimic the human arm. Motor systems depend on the laws of movement with the position of the arm controlled according to the function [29]-[32].

The theory of dynamic examples. For every function there is a suitable path. The arm must be designed to follow this path in the correct manner, which requires building and designing a model and conducting tests that verify the model's effectiveness in performing with high precision and efficiency [33]-[36].

Requirements for building a simulation model: creating a dynamic model that simulates the human arm. Build a path that fits the job that fits this model. Simulating the exoskeleton with a metal structure. Determine the structure's movement model by employing a machine that provides the required movement using the electric motor. Multiple sources of movement mean multiple machines, i.e. electric motors. Developing the appropriate algorithm for the path of movement of the arm, specifying the angles of each machine or motor, updating them with the change of time, and modifying the movement of the arm according to the path drawn to complete the required function. It is also necessary to conduct appropriate analysis for each simulation process according to different tests and different operating conditions [37]-[40].

3. Simulation Models and Results of DCM for Robotic Arm System

The current simulation involves building a model of a robot arm joint that moves with the help of an electric motor. The joint can move at a certain angle and then return to its previous position, which is a proposed test case. The joint can also perform two or three movements, which are other proposed test cases. The tests included simulating the movement of a joint using a simulation model that is selected with a reference signal with a unit value as a per-unit system. After verifying the usability of the model, a position with an angle of 60 degrees was chosen in a single-motion test. Two movements were chosen for a second test case using reference angles for two positions with angles of 60 degrees and 80 degrees in a test for more than one movement. Third, a test case for several movements and positions represented by angles of 40 degrees, 60 degrees, and 20 degrees. The simulation was conducted to verify the effectiveness of the system and to know the behavior of the system in different system cases, including the open-loop system, the closed-loop system without any control unit, and finally the closed-loop system with a traditional control unit. The results of the system

indicate the possibility of improving performance through traditional measurement criteria, which represent the response speed in the time of stability, transient, ascent, overshoot, and undershoot. The progress in modern technology includes many fields, some of which are related to robotics and its various applications, including medical applications that care for stroke patients. Health institutions and companies interested in this field can be helped by developing studies on these systems and working on designing advanced models with high reliability, safety and high efficiency. Open loop system simulation models, the first test case according to the unit system, the reference value for the angle at which the joint moves to a position with an angle of reference value of 1. The value is modified to the angle in degrees in the second test. While in other tests, it is suggested to move the arm to more than one position at different angles, including three suggestions represented by a movement at an angle of 60 degrees and returning to the previous position at an angle of zero. After that, two cases were tested for five equal periods of time at positions of different angles, as 40 degrees, 60 degrees, 20 degrees, and 80 degrees were suggested in addition to an angle of 0 degrees. In this section there are two parts, modeling of DCM and system results:

3.1. Simulation Models of DCM for Robotic Arm System

In this section there are three cases, Open-Loop System, Closed-Loop System without Controller and Closed-Loop System with Controller [41]-[53].

3.1.1. Open-Loop System

The first stage of testing the system using the DCM simulation model for the open loop system: In which a system is built and designed through which a basic performance of the system behavior is created in a state without feedback control. The system model can be displayed as in Fig. 5, Fig. 6, Fig. 7 and represents the block model and the MATLAB m file implementation model of the system.

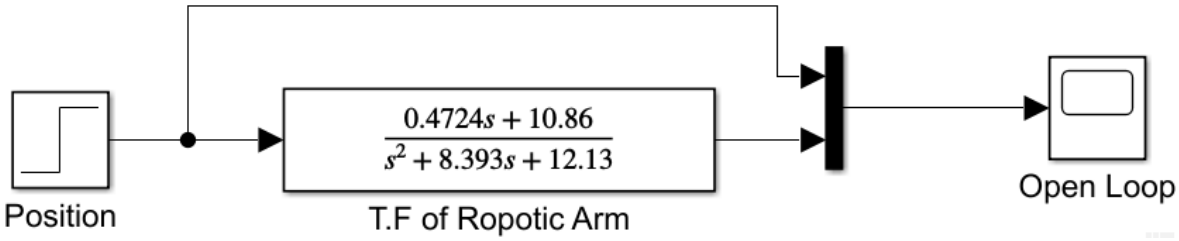

Fig. 5. Open loop simulation model of robot arm system with one position at different angles

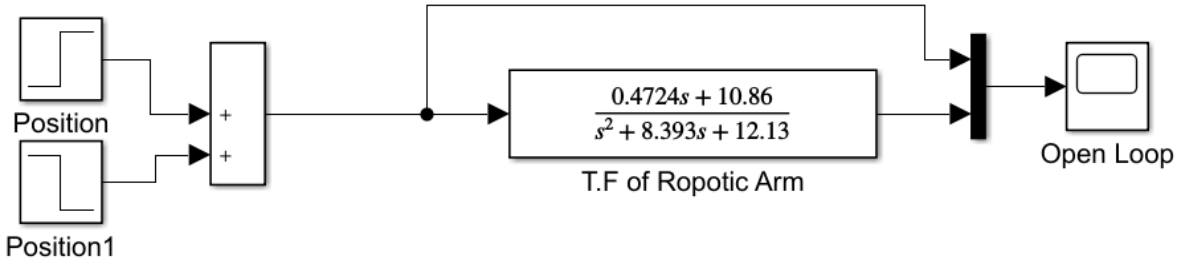

Fig. 6. Open loop simulation model of robot arm system with positions of an angle of 60 degrees and returning to the previous position at an angle of zero

3.1.2. Closed-Loop System without Controller

The second stage of testing the system using the DCM simulation model for the closed loop system is also without a control unit and contains feedback and this stage does not include any additional control mechanisms. The system model can be displayed as in Fig. 8, Fig. 9, Fig. 10 Preparing the model.

3.1.3. Closed-Loop System with Controller

The third stage of testing the system using the DCM simulation model for the closed loop system with a control unit in order to obtain an improvement in performance. The system model can be

displayed as in Fig. 11, Fig. 12, Fig. 13 and it contains the block diagram in addition to the MATLAB m file where the PID controller has been integrated to implement the system model with the traditional PIDC controller.

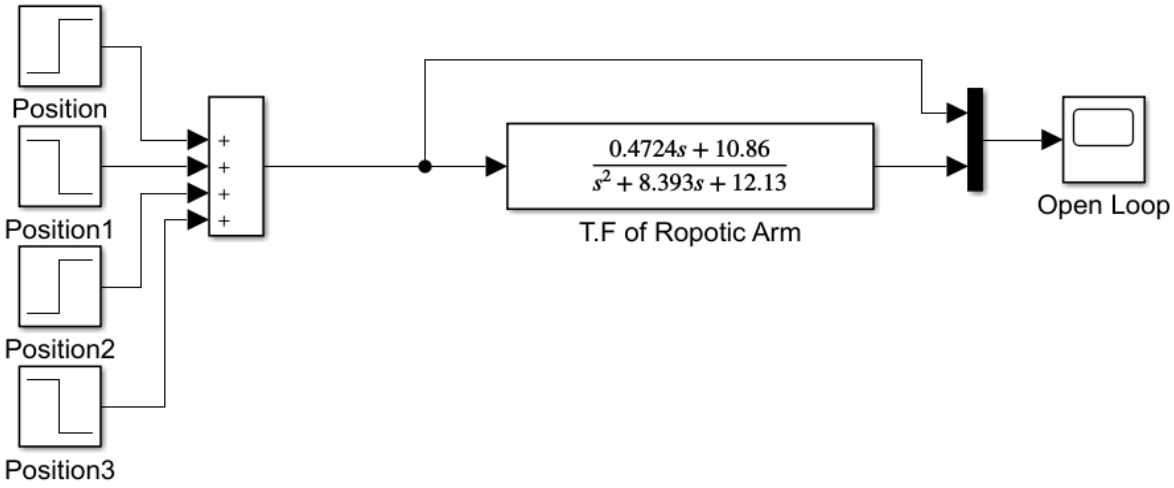

Fig. 7. Open loop simulation model of robot arm system with positions of different angles, as 40 degrees, 60 degrees, 20 degrees, and 80 degrees

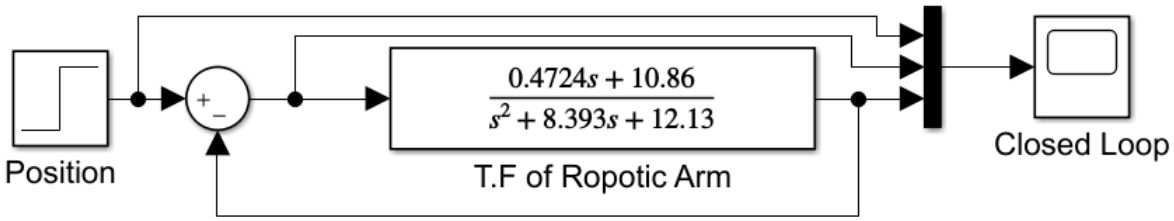

Fig. 8. Closed loop simulation model without controller of robot arm system with one position

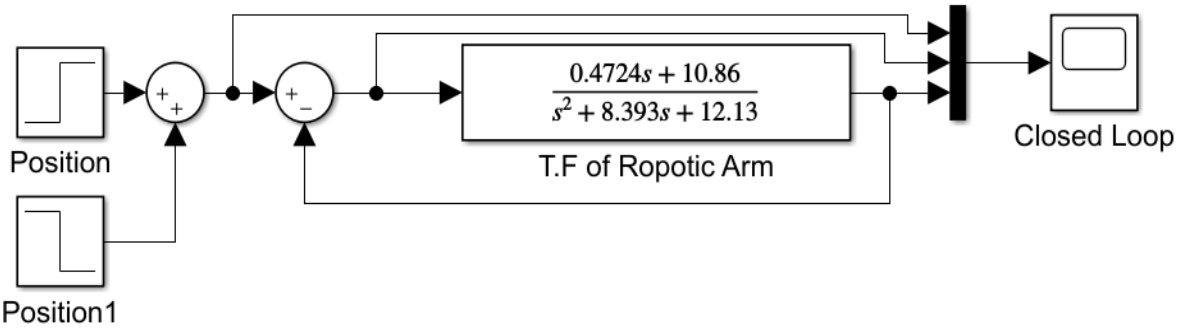

Fig. 9. Closed loop simulation model without controller of robot arm system with positions of an angle of 60 degrees and returning to the previous position at an angle of zero

The third stage of simulation is to use simulation models based on the transfer function of the open-loop and closed-loop system and the conventional controller as in the simulation model of the Fig. 11, Fig. 12, Fig. 13).

3.2. System Results of DCM for Robotic Arm System

In this section there are three cases, Open-Loop System, Closed-Loop System without Controller and Closed-Loop System with Controller.

3.2.1. Results for Open-Loop System

After conducting the first test to simulate the system using the open loop system model, the results of this stage indicate what is shown in Fig. 14, Fig. 15, Fig. 16, which represents the performance

response of the system model simulation in the basic open loop configuration without any control mechanisms.

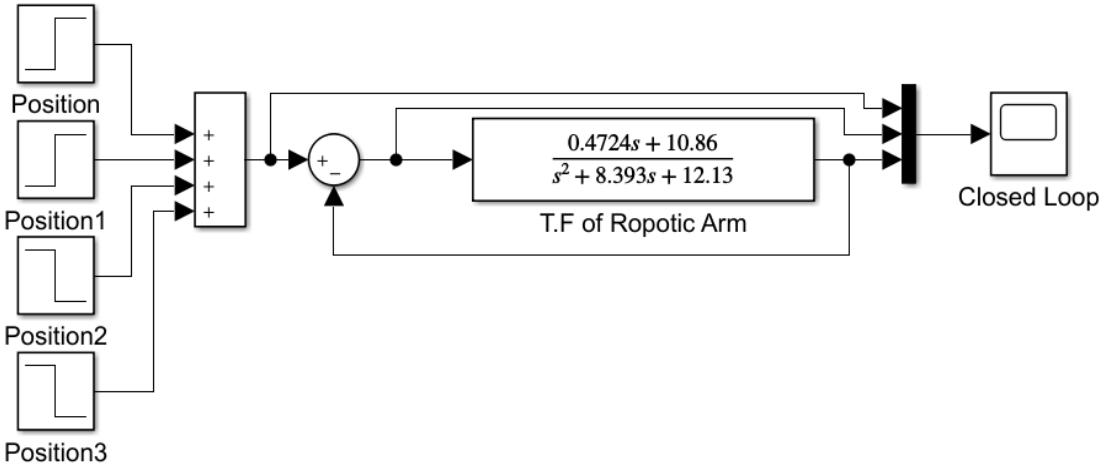

Fig. 10. Closed loop simulation model without controller of robot arm system with positions of different angles, as 40 degrees, 60 degrees, 20 degrees, and 80 degrees

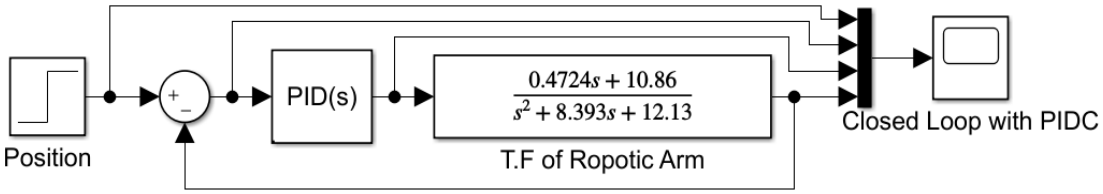

Fig. 11. Closed loop simulation model with conventional PID controller of robot arm system with one position at different angles

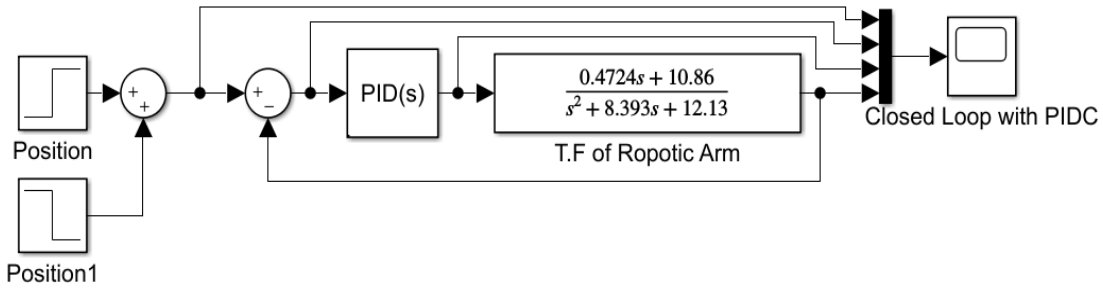

Fig. 12. Closed loop simulation model with conventional PID controller of robot arm system with positions of an angle of 60 degrees and returning to the previous position at an angle of zero

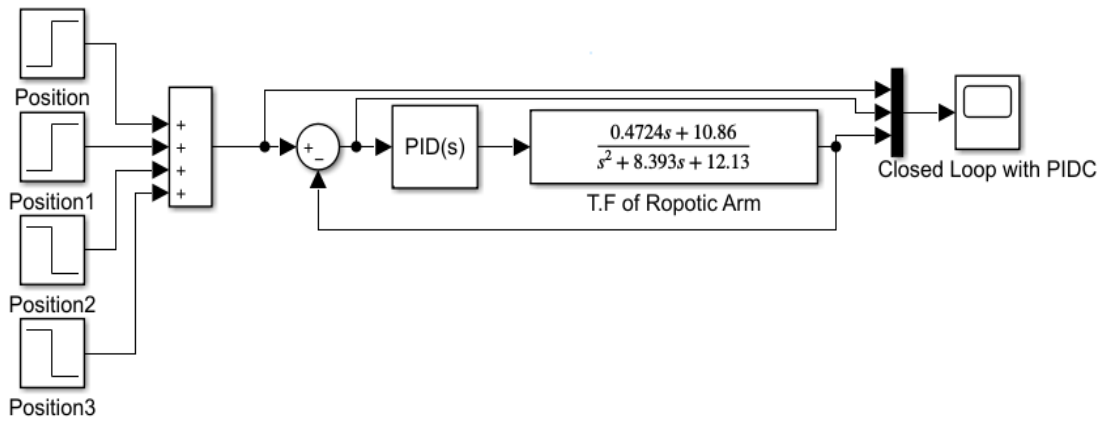

Fig. 13. Closed loop simulation model with conventional PID controller of robot arm system with positions of different angles, as 40 degrees, 60 degrees, 20 degrees, and 80 degrees

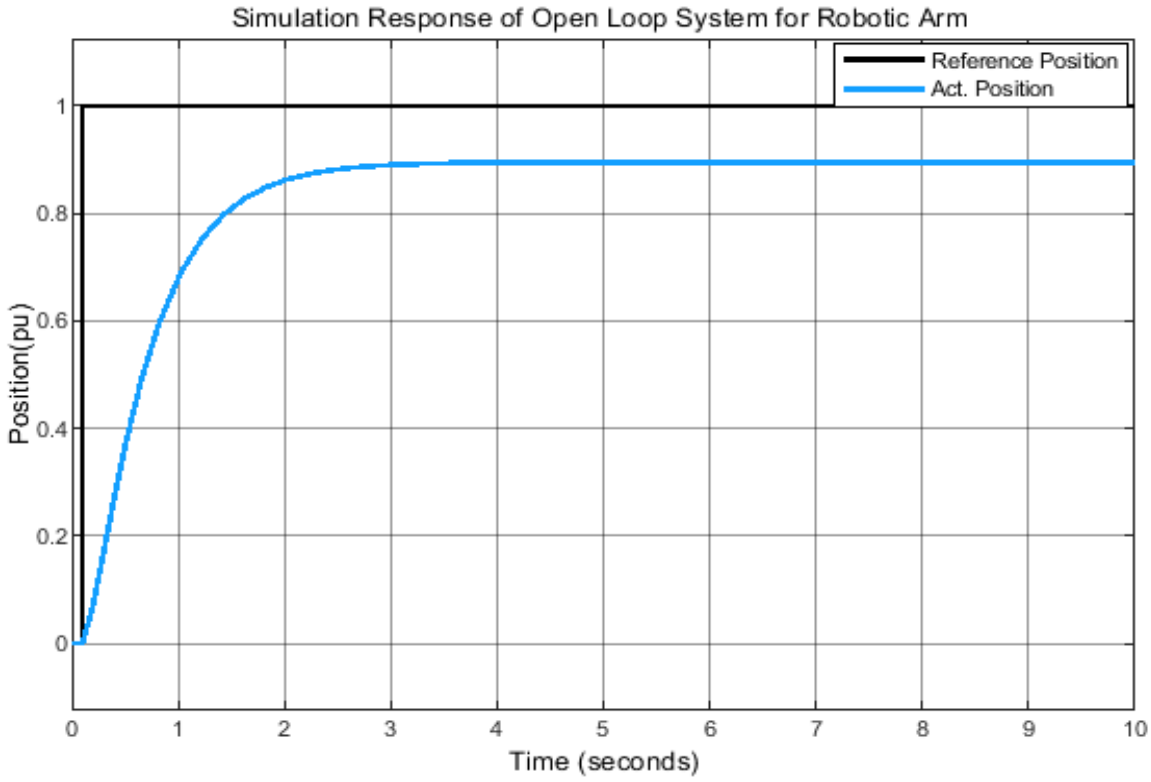

(a) Position in (pu)

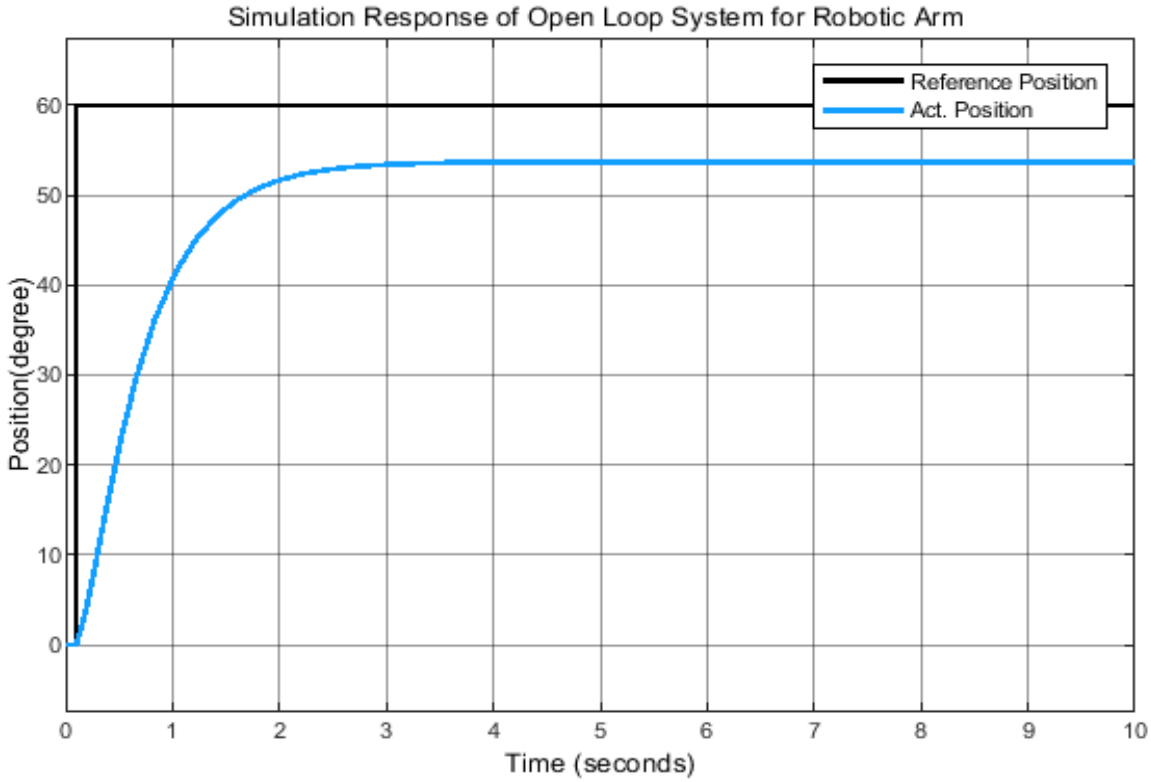

(b) Position in (degree)

Fig. 14. Open loop simulation result of robot arm system with one position at different angles

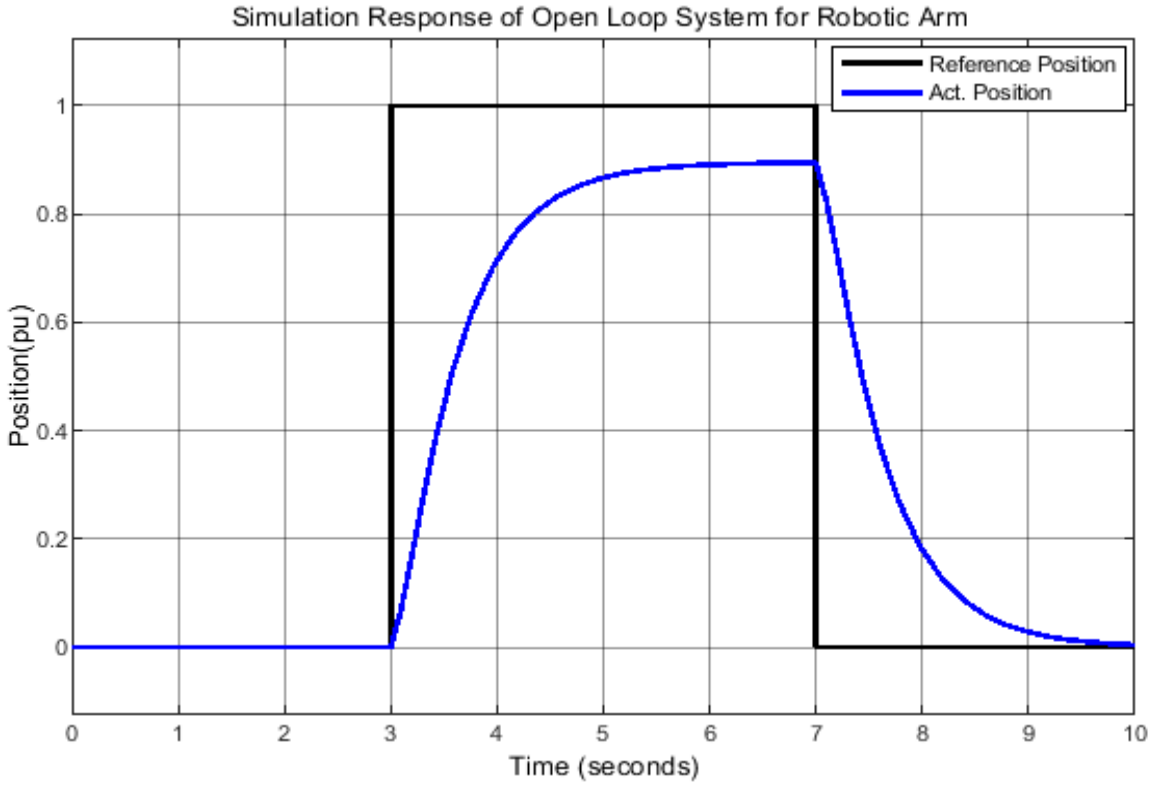

(a) Position in (pu)

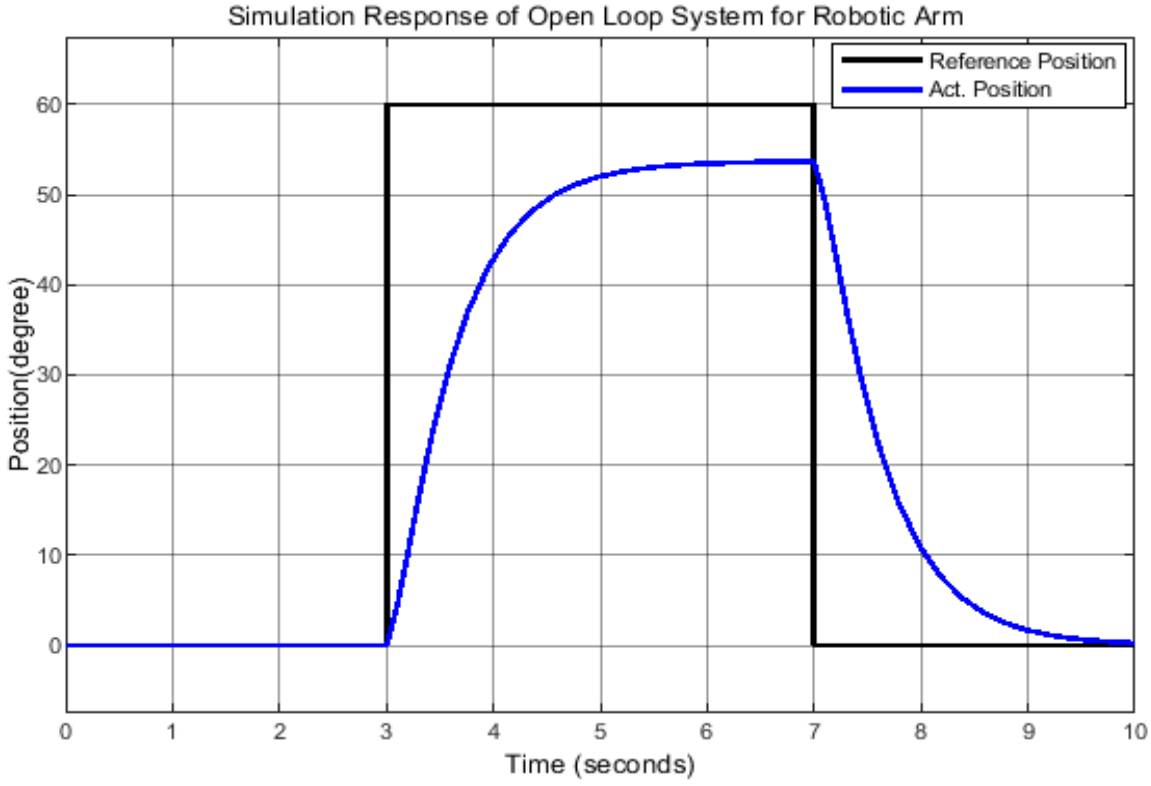

(b) Position in (degree)

Fig. 15. Open loop simulation model of robot arm system with positions of an angle of 60 degrees and returning to the previous position at an angle of zero

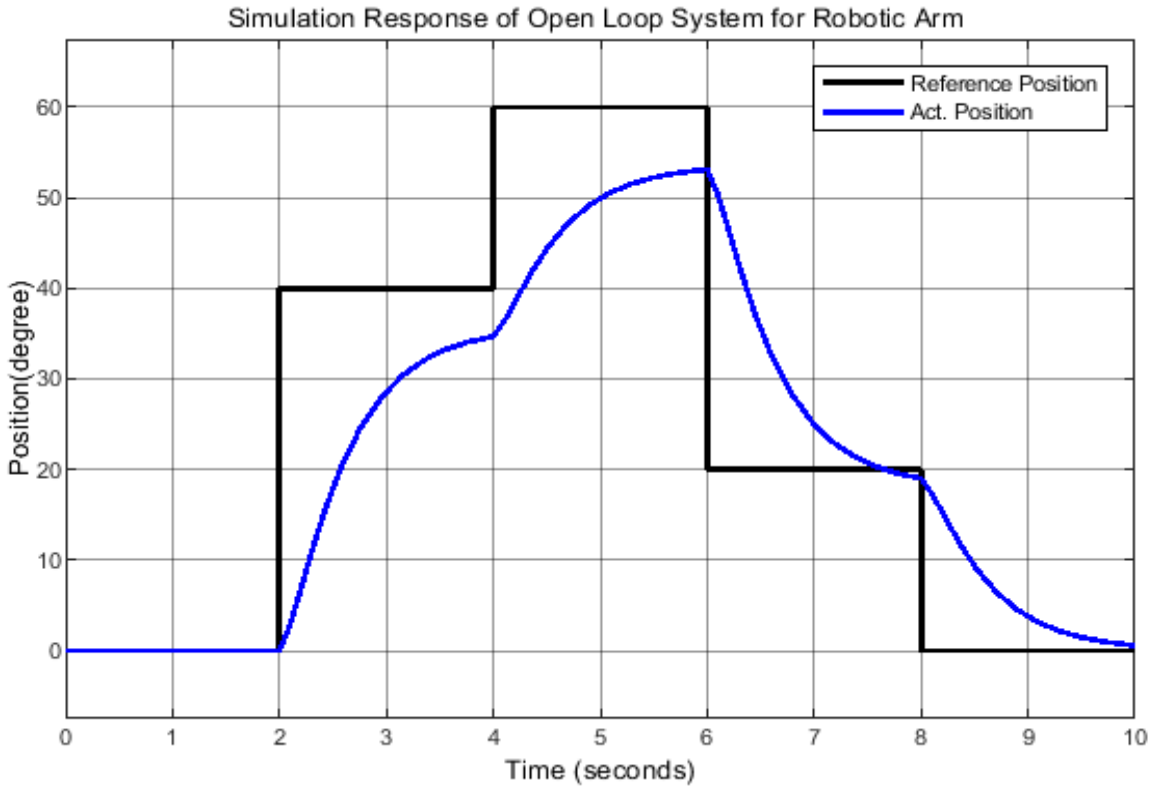

(a) Position in (0,40,60,20,0) degrees

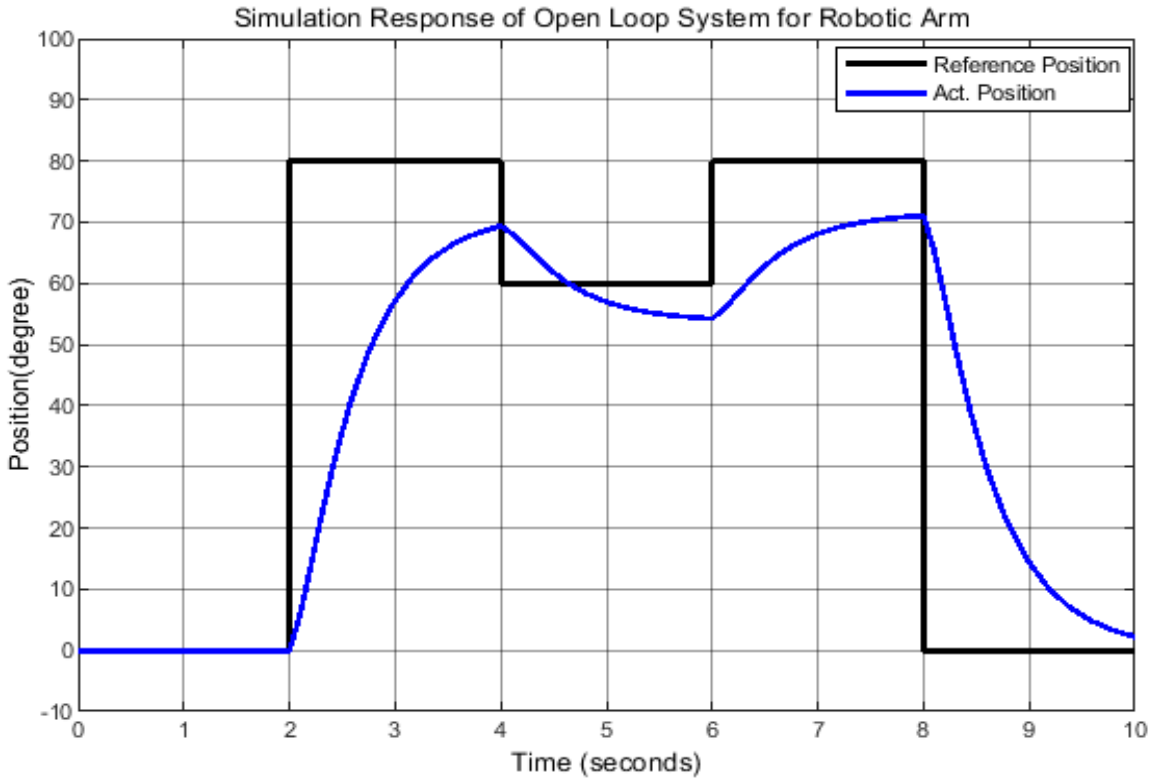

(b) Position in (0,80,60,80,0)degrees

Fig. 16. Open loop simulation model of robot arm system with positions of different angles, as 40 degrees, 60 degrees, 20 degrees, and 80 degrees

3.2.2. Results for Closed-Loop System without Controller

After conducting the second test to simulate the system using the closed loop system model without additional control, the results of this stage indicate what is shown in Fig. 17, Fig. 18, which represents the response of the closed loop system, in addition to highlighting the change in performance.

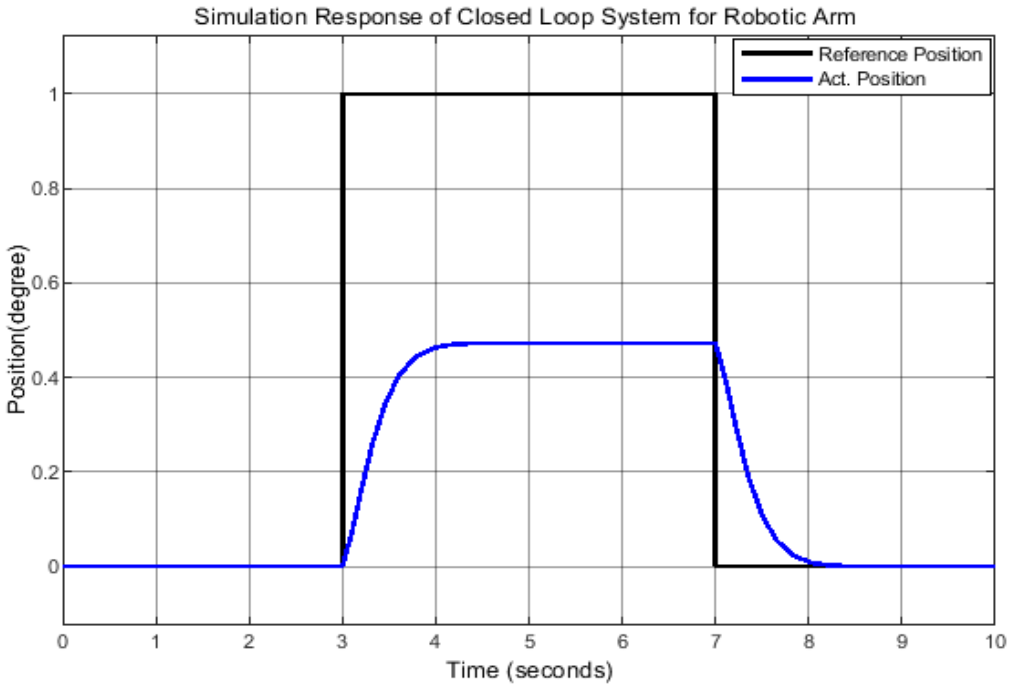

(a) Position in (pu)

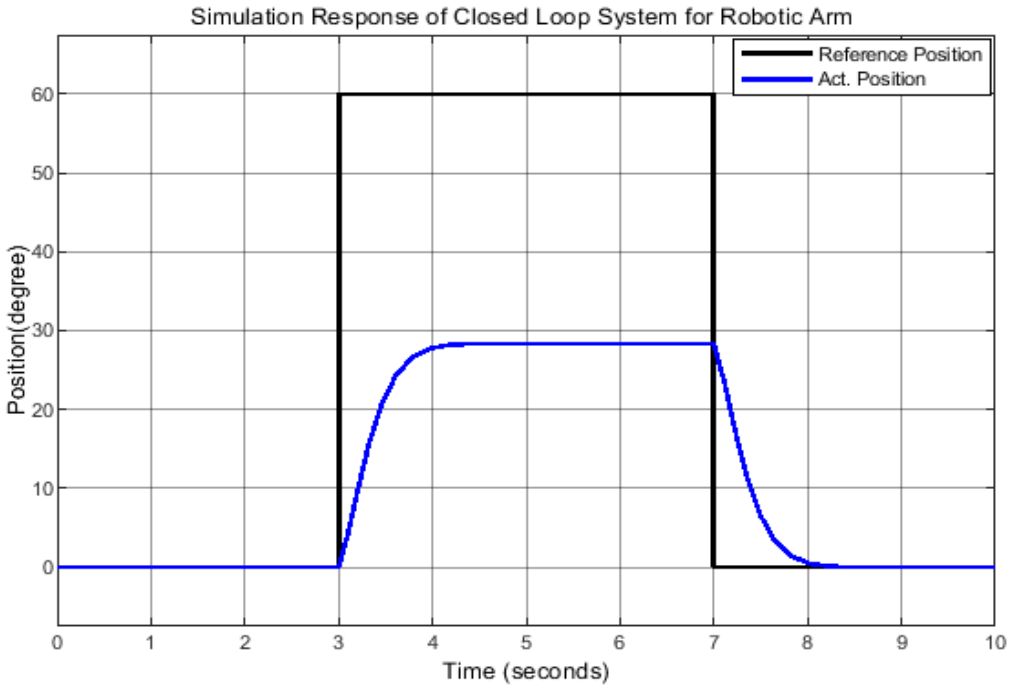

(b) Position in (degree)

Fig. 17. Closed loop simulation model of robot arm system with positions of an angle of 60 degrees and returning to the previous position at an angle of zero

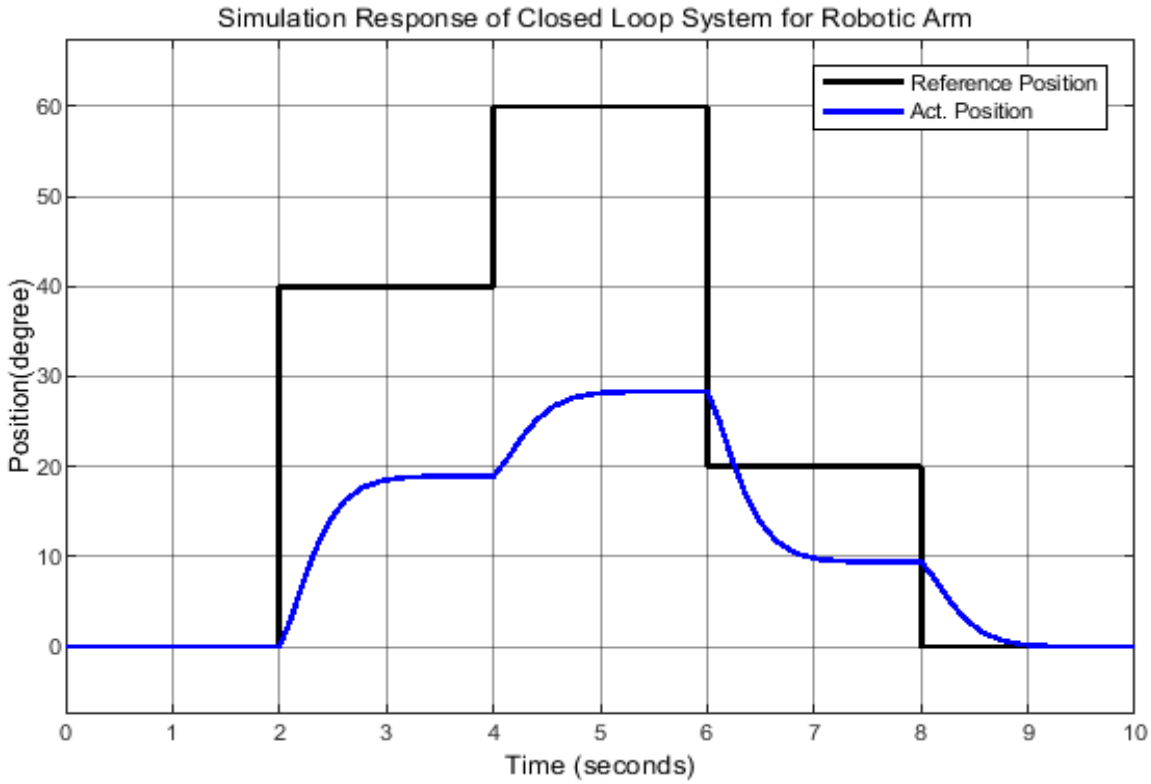

(a) Position in (0,40,60,20,0) degrees

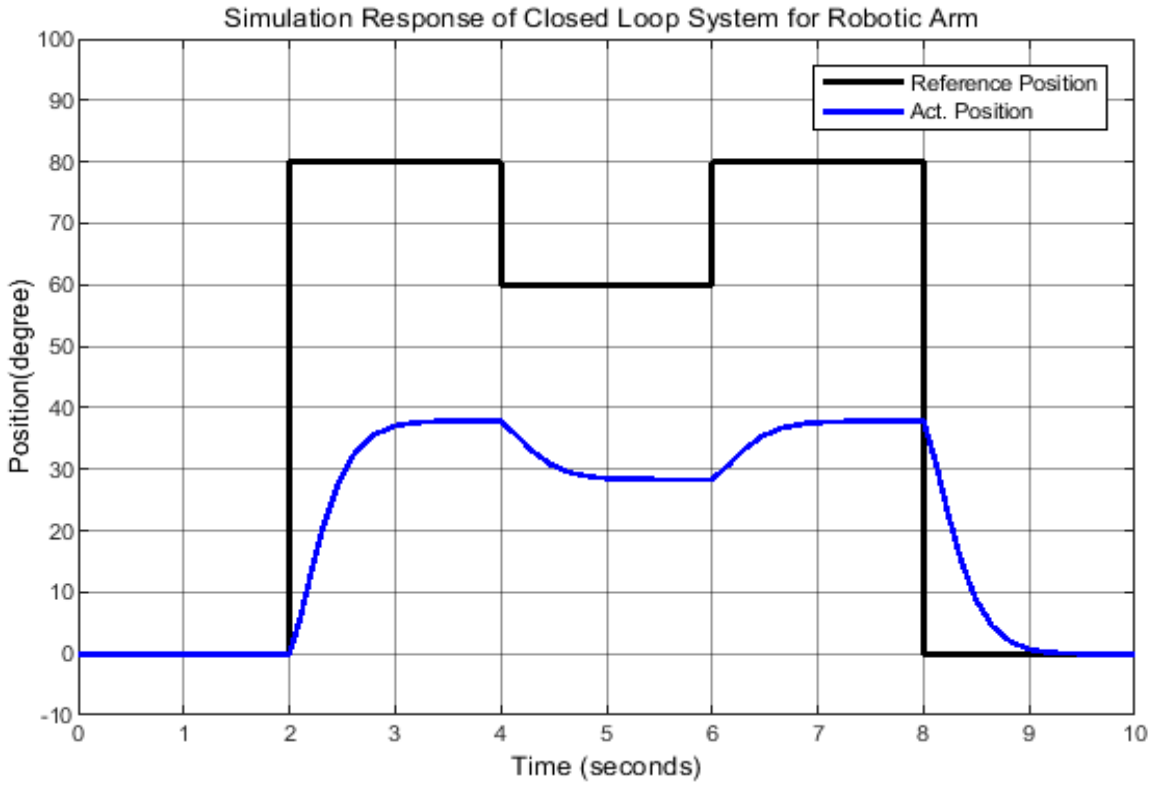

(b) Position in (0,80,60,80,0)degrees

Fig. 18. Closed loop simulation model of robot arm system with positions of different angles, as 40 degrees, 60 degrees, 20 degrees, and 80 degrees

3.2.3. Results for Closed-Loop System with PIDC

After conducting the second test to simulate the system using the closed loop system model with PIDC, the results of this stage indicate what is shown in Fig. 19, Fig. 20, Fig. 21, the results for the closed loop system with PIDC. This shows the clear improvements in the system response to the outputs of the simulation process.

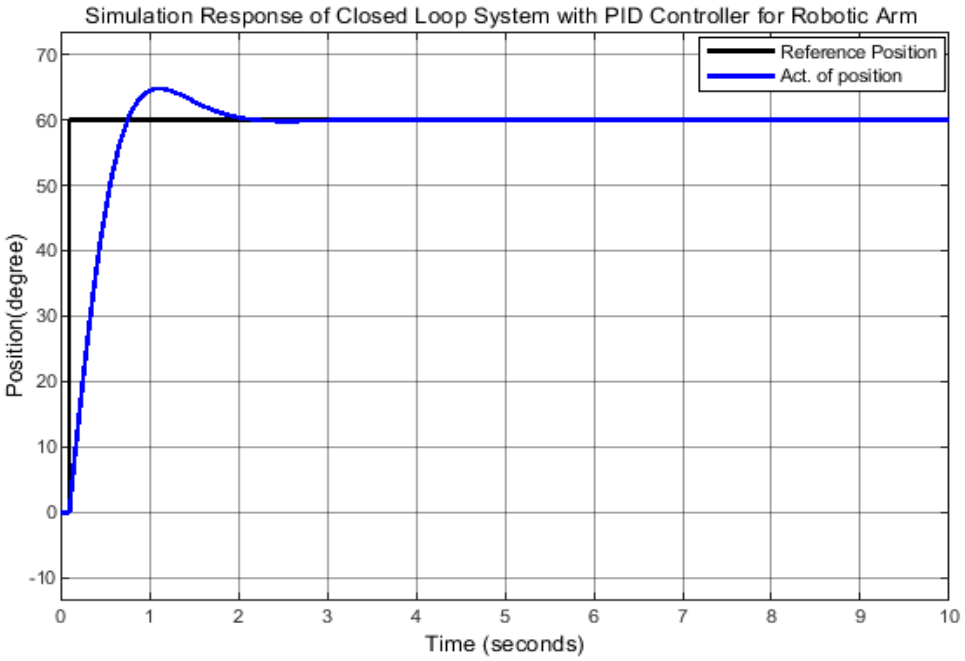

(a) Position in (pu)

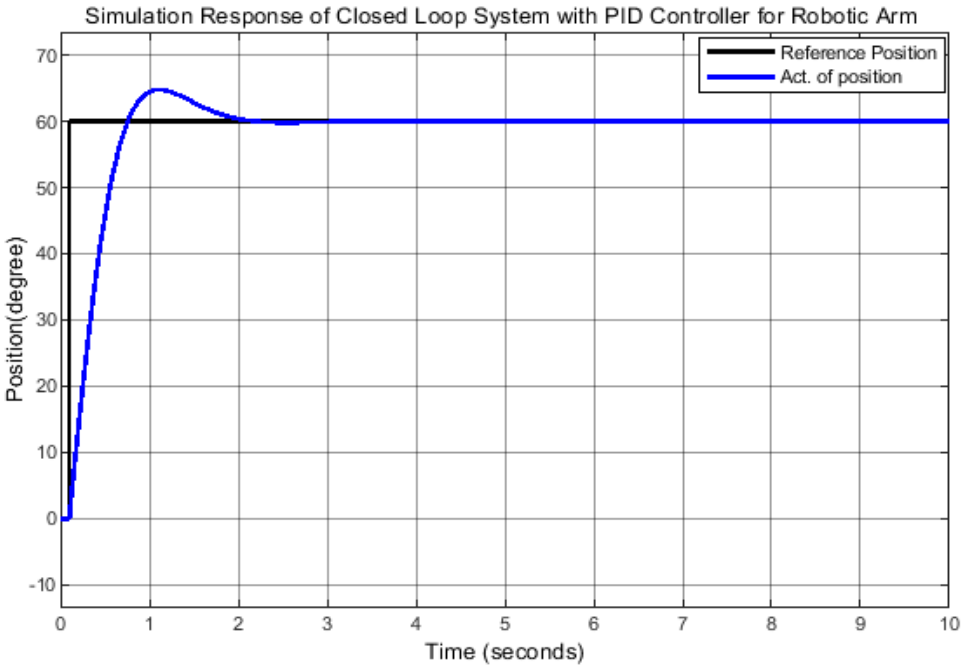

(b) Position in (degree)

Fig. 19. Closed loop simulation model with conventional PID controller of robot arm system with one position at different angles

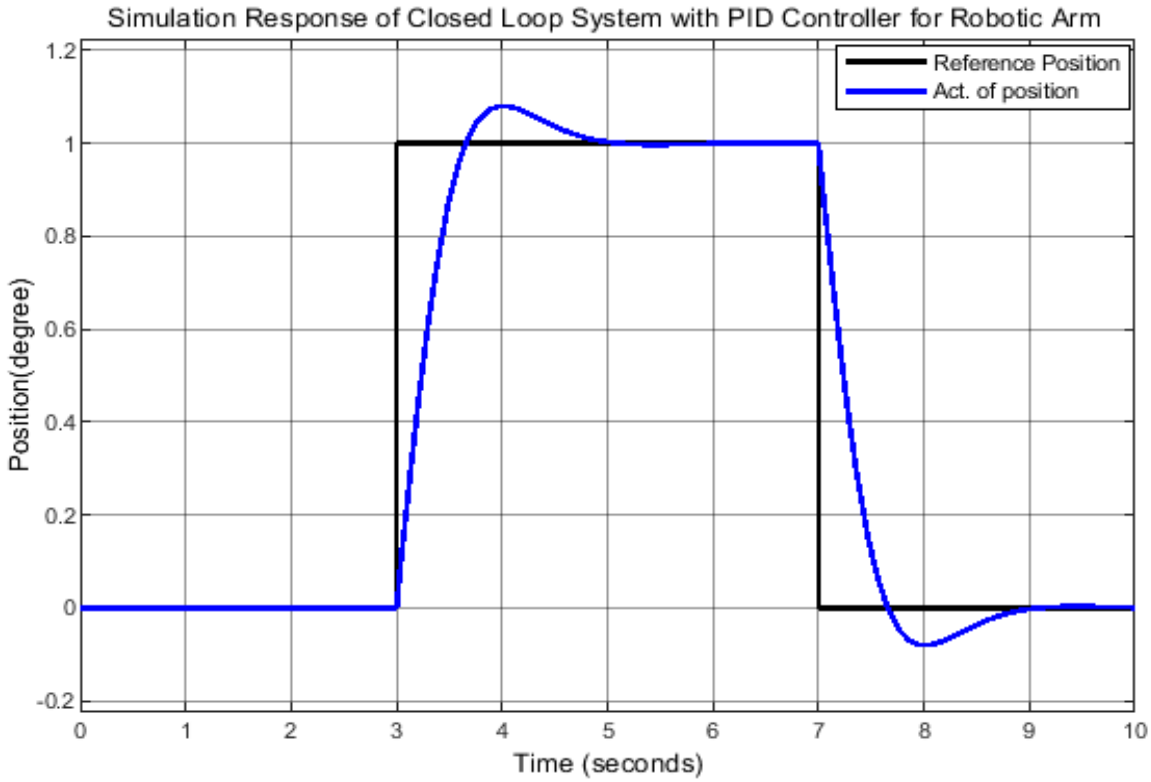

(a) Position in (pu)

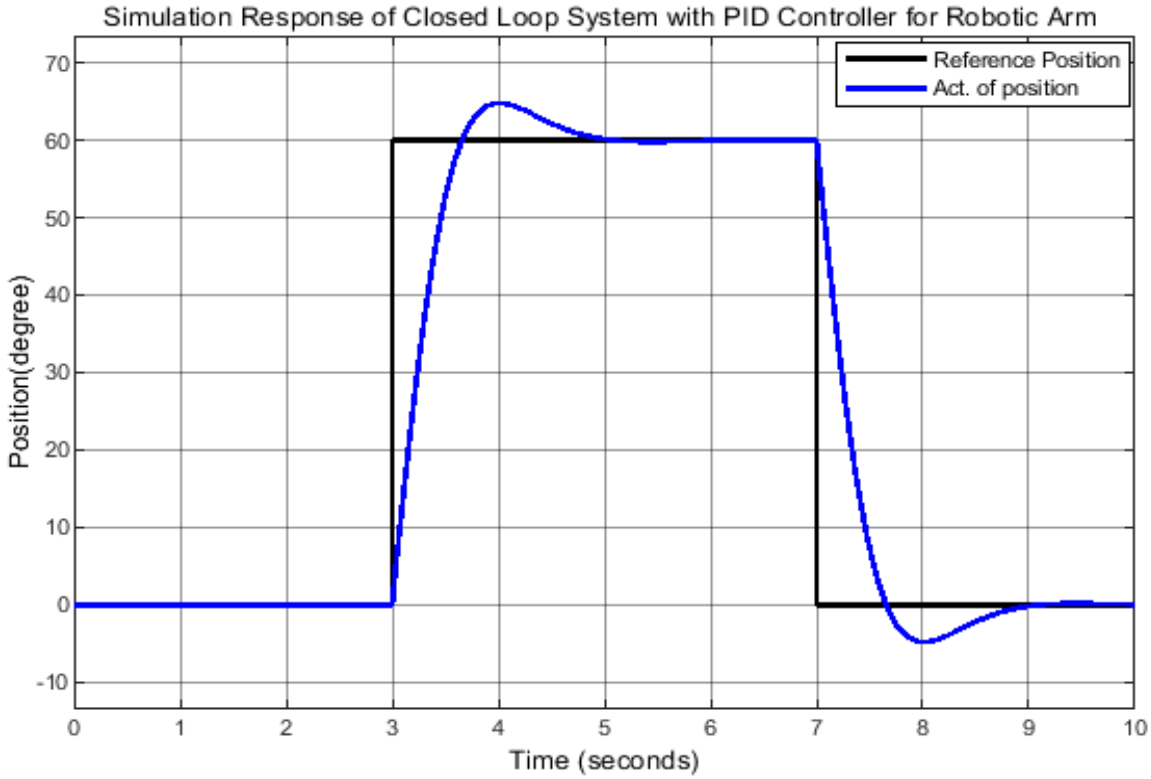

(b) Position in (degree)

Fig. 20. Closed loop simulation model with conventional PID controller of robot arm system with positions of an angle of 60 degrees and returning to the previous position at an angle of zero

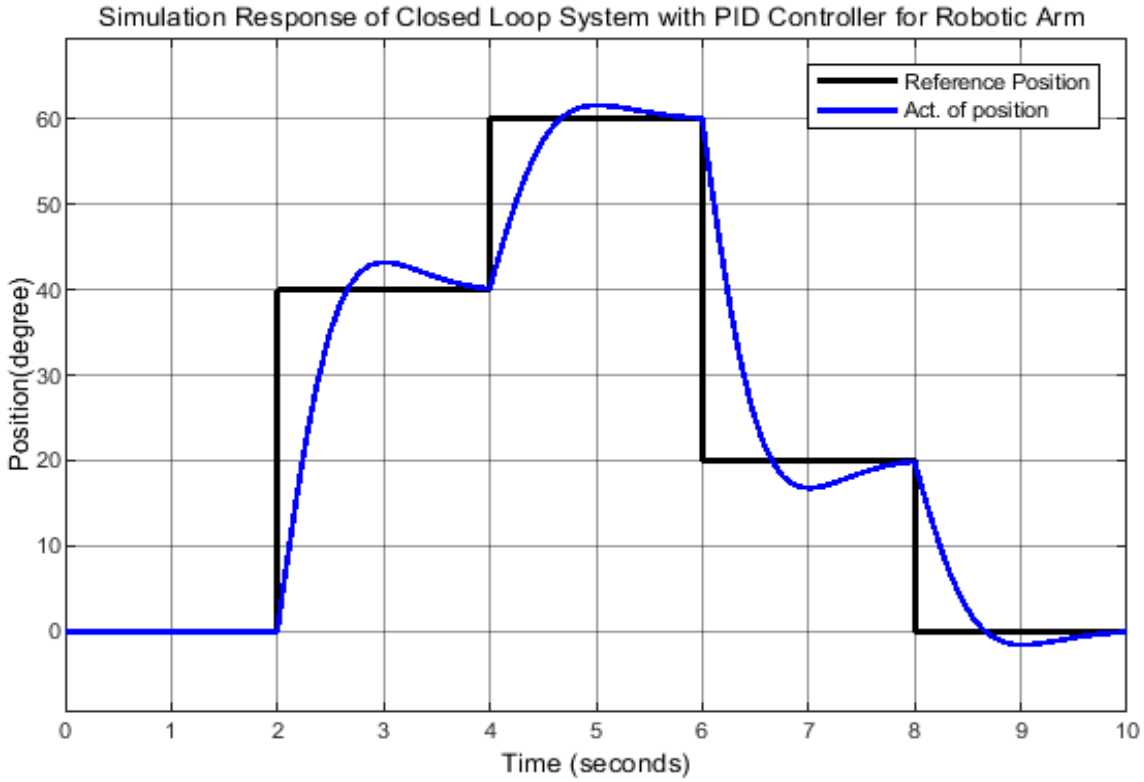

(a) Position in (0,40,60,20,0) degrees

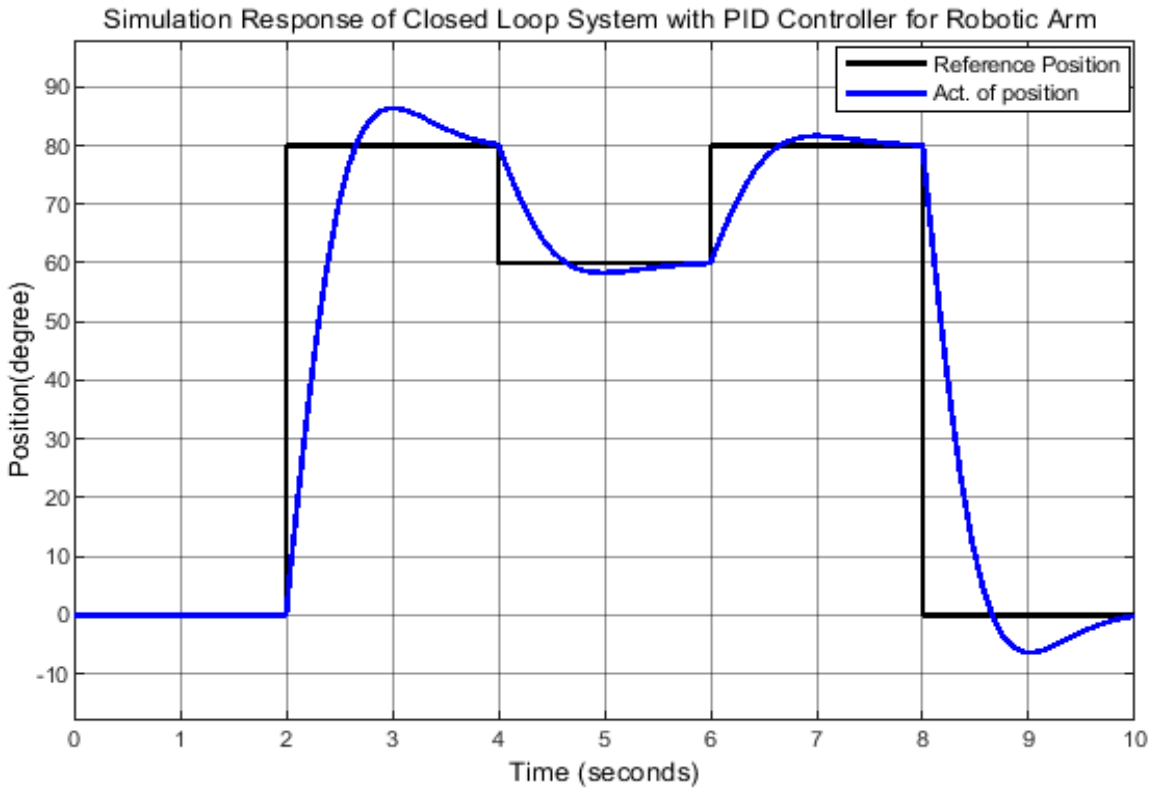

(b) Position in (0,80,60,80,0)degrees

Fig. 21. Closed loop simulation model with conventional PID controller of robot arm system with positions of different angles, as 40 degrees, 60 degrees, 20 degrees, and 80 degrees

The simulation results indicate the performance measurement criteria with the appropriate parameter values that were adopted in the case of control using the conventional controller, as in the Fig. 22.

Controller Parameters

	Tuned	Block
P	2.0807	2.0807
I	5.4975	5.4975
D	0.10953	0.10953
N	34.2066	34.2066

Performance and Robustness

	Tuned	Block
Rise time	0.479 seconds	0.479 seconds
Settling time	1.67 seconds	1.67 seconds
Overshoot	8.01 %	8.01 %
Peak	1.08	1.08
Gain margin	Inf dB @ NaN rad/s	Inf dB @ NaN rad/s
Phase margin	69 deg @ 3.26 rad/s	69 deg @ 3.26 rad/s
Closed-loop stability	Stable	Stable

Fig. 22. The firs sample of tuning for PIDC

The upper part of the Fig. 22 indicates the values of the parameters of the traditional controller, which included all of the P=2.0807, I=5.4975 and D=0.10953, while the other part indicates the performance measures, which were represented by, Rise time is equal 0.479sec, settling time is equal 1.67sec and overshoot is equal 8.01%.

The upper part of the Fig. 23 indicates the values of the parameters of the traditional controller, which included all of the P=1.657, I=3.5334 and D=0.071242, while the other part indicates the performance measures, which were represented by, Rise time is equal 0.653sec, settling time is equal 2.3sec and overshoot is equal 7.78%.

The upper part of the Fig. 24 indicates the values of the parameters of the traditional controller, which included all of the P=1.5736, I=3.01512 and D=0.0559, while the other part indicates the performance measures, which were represented by, Rise time is equal 0.734sec, settling time is equal 2.59sec and overshoot is equal 7.41%.

Simulation is the use of simulation models based on the open-loop and closed-loop system transfer function and the traditional controller as in simulation models. After conducting tests to simulate the system using open-loop and closed-loop models with and without PIDC, the simulation results can be obtained, which represent the system response. The results for the closed-loop system with PIDC show a clear improvement in the system response to the simulation process outputs. The simulation uses the arm to perform different movements at angles according to the application, including first moving the first joint at one angle and testing another at more than one angle. The simulation of the performance of some robotic arm movements also includes different movements according to the joint and the angle to be modified and the appropriate time to perform those movements. Different movements can be set for each joint, including one or more movements for each joint at a fixed or variable angle. The simulation model for robotic arm movements includes three models, the first is open loop without a feedback signal. The second is closed loop without a controller. The third is closed loop with a PID controller. The simulation results for robotic arm movements include three models, the first is open loop without a feedback signal. The second is closed loop without a controller. The third is a closed loop with a PID controller. One of the proposed tests is to

run three periods of ten seconds total divided into three periods: a three-second first period, a four-second second period, and a three-second third period. The first period is a stable angle at the previous state, i.e. without change, so zero degrees appear in the first period. In the second period, the arm moves at an angle of 60 degrees from the previous one. Finally, the third movement is at an angle of -60 degrees. In the same way, different models can be used to represent all joints and perform movements simultaneously.

Controller Parameters

	Tuned	Block
P	1.657	1.657
I	3.5334	3.5334
D	0.071242	0.071242
N	271.7298	271.7298

Performance and Robustness

	Tuned	Block
Rise time	0.653 seconds	0.653 seconds
Settling time	2.3 seconds	2.3 seconds
Overshoot	7.78 %	7.78 %
Peak	1.08	1.08
Gain margin	Inf dB @ NaN rad/s	Inf dB @ NaN rad/s
Phase margin	69 deg @ 2.38 rad/s	69 deg @ 2.38 rad/s
Closed-loop stability	Stable	Stable

Fig. 23. The second sample of tuning for PIDC

Controller Parameters

	Tuned	Block
P	1.5736	1.5736
I	3.0512	3.0512
D	0.0559	0.0559
N	239.6011	239.6011

Performance and Robustness

	Tuned	Block
Rise time	0.734 seconds	0.734 seconds
Settling time	2.59 seconds	2.59 seconds
Overshoot	7.41 %	7.41 %
Peak	1.07	1.07
Gain margin	Inf dB @ NaN rad/s	Inf dB @ NaN rad/s
Phase margin	69 deg @ 2.1 rad/s	69 deg @ 2.1 rad/s
Closed-loop stability	Stable	Stable

Fig. 24. The third sample of tuning for PIDC

There are also five periods of ten seconds total divided into equal periods. The first period is a stable angle at the previous state, i.e. without change, so zero degrees appear in the first period. The second period is the arm movement at an angle of 40 degrees from the previous one, the third 60

degrees, the fourth 20 degrees, and finally the fifth movement at an angle of -20 degrees. Another test case is to run five periods of ten seconds total divided into equal periods including the first period is a stable angle at the previous state, i.e. without change, so zero degrees appear in the first period. The second period is the arm movement at an angle of 80 degrees from the previous one, the third 60 degrees, the fourth 80 degrees, and finally the fifth movement at an angle of -80 degrees.

4. Conclusion

The proposed tests were conducted in two stages, including the prototype building stage, which was used to verify the effectiveness of the system and the possibility of simulating and operating the model to determine the system behavior. The possibility of operating the arm joints for periods of time and at multiple angles was also verified to determine the system behavior in terms of performance speed and response. The verification was conducted by conducting more than one test and for an operating period divided into periods that fit the proposed tests. The possibility of improving the performance was verified using the conventional controller. In this study, a PID controller model was presented and implemented to improve the performance of the motion system of the robotic arm used for upper limb rehabilitation for stroke patients. The effectiveness of the presented model was verified by comparing two cases of the system without a PID controller and an open-loop system. A control system for an articulated robotic arm was developed by simulating this arm using MATLAB to perform precise movements based on the PID controller proposed in this research to perform precise movements along a pre-defined path, suitable for various industrial applications.

Author Contribution: All authors contributed equally to the main contributor to this paper. All authors read and approved the final paper.

Funding: This research received no external funding.

Conflicts of Interest: The authors declare no conflict of interest.

References

[1] R. Chotikunnan, K. Roongprasert, P. Chotikunnan, P. Imura, M. Sangworasil, A. Srisiriwat, "Robotic Arm Design and Control Using MATLAB/Simulink," *International Journal of Membrane Science and Technology*, vol. 10, no. 3, pp. 2448-2459, 2023, https://www.cosmosscholars.com/phms/index.php/ijmst/article/view/1974/1275.

[2] J. A. G. L. Junior, J. M. Balthazar, M. A. Ribeiro, F. C. Janzen, A. M. Tusset, "Dynamic model of a robotic manipulator with one degree of freedom with friction component," *International Journal of Robotics and Control Systems*, vol. 3, no. 2, pp. 315-329, 2023, https://doi.org/10.31763/ijrcs.v3i2.984.

[3] F. Ahmmed, "Arduino-Controlled Multi-Function Robot with Bluetooth and nRF24L01+ Communication," *International Journal of Robotics and Control Systems*, vol. 4, no. 3, pp. 1353-1381, 2024, https://doi.org/10.31763/ijrcs.v4i3.1517.

[4] D. Prasetiyo and W. S. Aji, "Irrigation Sluice Control System Using Algorithm Based DC Motor PID And Omron PLC," *Control Systems and Optimization Letters*, vol. 1, no. 1, pp. 19-26, 2023, https://doi.org/10.59247/csol.v1i1.5.

[5] Z. B. Abdullah, S. H. Dakheel, and S. W. Shneen, "Simulation model of using ANN and PID controller for 2Ph-HSM by matlab," *AIP Conference Proceedings*, vol. 3002, no. 1, p. 050004, 2024, https://doi.org/10.1063/5.0206748.

[6] V. K. Munagala and R. K. Jatoth, "A novel approach for controlling DC motor speed using NARXnet based FOPID controller," *Evolving Systems*, vol. 14, no. 1, pp. 101–116, 2023, https://doi.org/10.1007/s12530-022-09437-1.

[7] S. W. Shneen, A. L. Shuraiji, K. R. Hameed, "Simulation model of proportional integral controller-PWM DC-DC power converter for DC motor using matlab," *Indonesian Journal of Electrical Engineering and Computer Science*, vol. 29, no. 2, pp. 725-734, 2023, http://doi.org/10.11591/ijeecs.v29.i2.pp725-734.

[8] D. Saputra, A. Ma'arif, H. Maghfiroh, P. Chotikunnan, S. N. Rahmadhia, "Design and application of PLC-based speed control for DC motor using PID with identification system and MATLAB tuner," *International Journal of Robotics and Control Systems*, vol. 3, no. 2, pp. 233-244, 2023, https://doi.org/10.31763/ijrcs.v3i2.775.

[9] J. Laarni, H. Koskinen, and A. Väätänen, "Concept of operations as a boundary object for knowledge sharing in the design of robotic swarms," *International Journal of Robotics and Control Systems*, vol. 2, no. 4, pp. 692-708, 2022, https://doi.org/10.31763/ijrcs.v2i4.834.

[10] J. Mellado and F. Núñez, "Design of an IoT-PLC: A containerized programmable logical controller for the industry 4.0," *Journal of Industrial Information Integration*, vol. 25, p. 100250, 2022, https://doi.org/10.1016/j.jii.2021.100250.

[11] S. W. Shneen, H. S. Dakheel, and Z. B. Abdullah, "Design and Implementation of No Load, Constant and Variable Load for DC Servo Motor," *Journal of Robotics and Control (JRC)*, vol. 4, no. 3, pp. 323-329, 2023, https://doi.org/10.18196/jrc.v4i3.17387.

[12] S. S. Khairullah and A. N. Sharkawy, "Design and Implementation of a Reliable and Secure Controller for Smart Home Applications Based on PLC," *Journal of Robotics and Control (JRC)*, vol. 3, no. 5, pp. 614–621, 2022, https://doi.org/10.18196/jrc.v3i5.15972.

[13] A. Rajagukguk, W. Arafanaldy, A. Anhar, and N. Nurhalim, "Pitch Blade Control Prototype Design for Vertical Axis Wind Power Plant," *Jurnal Ilmiah Teknik Elektro Komputer dan Informatika*, vol. 8, no. 1, pp. 157–166, 2022, https://doi.org/10.26555/jiteki.v8i1.23662.

[14] P. Sutyasadi, "Control Improvement of Low-Cost Cast Aluminium Robotic Arm Using Arduino Based Computed Torque Control," *Jurnal Ilmiah Teknik Elektro Komputer dan Informatika*, vol. 8, no. 4, pp. 650–659, 2022, https://doi.org/10.26555/jiteki.v8i4.24646.

[15] H. S. Dakheel, Z. B. Abdullah, and S. W. Shneen, "Advanced optimal GA-PID controller for BLDC motor," *Bulletin of Electrical Engineering and Informatics*, vol. 12, no. 4, pp. 2077-2086, 2023, https://doi.org/10.11591/eei.v12i4.4649.

[16] A. U. Nisa, S. Samo, R. A. Nizamani, A. Irfan, Z. Anjum, L. Kumar, "Design and Implementation of Force Sensation and Feedback Systems for Telepresence Robotic Arm," *Journal of Robotics and Control (JRC)*, vol. 3, no. 5, pp. 710-715, 2022, https://doi.org/10.18196/jrc.v3i5.15959.

[17] A. Kherkhar, Y. Chiba, A. Tlemçani, and H. Mamur, "Thermal investigation of a thermoelectric cooler based on Arduino and PID control approach," *Case Studies in Thermal Engineering*, vol. 36, p. 102249, 2022, https://doi.org/10.1016/j.csite.2022.102249.

[18] Z. B. Abdullah, S. W. Shneen, H. S. Dakheel, "Simulation model of PID controller for DC servo motor at variable and constant speed by using MATLAB," *Journal of Robotics and Control (JRC)*, vol. 4, no. 1, pp. 54-59, 2023, https://doi.org/10.18196/jrc.v4i1.15866.

[19] I. J. Meem, S. Osman, K. M. H. Bashar, N. I. Tushar, R. Khan, "Semi Wireless Underwater Rescue Drone with Robotic Arm," *Journal of Robotics and Control (JRC)*, vol. 3, no. 4, pp. 496-504, 2022, https://doi.org/10.18196/jrc.v3i4.14867.

[20] A. J. Attiya, S. W. Shneen, B. A. Abbas, Y. Wenyu, "Variable speed control using fuzzy-pid controller for two-phase hybrid stepping motor in robotic grinding," *Indonesian Journal of Electrical Engineering and Computer Science*, vol. 3, no. 1, pp. 102-118, 2016, http://doi.org/10.11591/ijeecs.v3.i1.pp102-118.

[21] E. S. Ghith, F. A. A. Tolba, "Design and Optimization of PID Controller using Various Algorithms for Micro-Robotics System," *Journal of Robotics and Control (JRC)*, vol. 3, no. 3, pp. 244-256, 2022, https://doi.org/10.18196/jrc.v3i3.14827.

[22] L. Yang, N. Guo, R. Sakamoto, N. Kato, K. Yano, "Electric wheelchair hybrid operating system coordinated with working range of a robotic arm," *Journal of Robotics and Control (JRC)*, vol. 3, no. 5, pp. 679-689, 2022, https://doi.org/10.18196/jrc.v3i5.15944.

[23] G. A. Aziz, S. W. Shneen, F. N. Abdullah, D. H. Shaker, "Advanced optimal GWO-PID controller for DC motor," *International Journal of Advances in Applied Sciences*, vol. 11, no. 3, pp. 263-276, 2022, http://doi.org/10.11591/ijaas.v11.i3.pp263-276.

[24] M. Filo, S. Kumar, and M. Khammash, "A hierarchy of biomolecular proportional-integral-derivative feedback controllers for robust perfect adaptation and dynamic performance," *Nature Communications*, vol. 13, no. 1, pp. 1–19, 2022, https://doi.org/10.1038/s41467-022-29640-7.

[25] S. Müftü, Said, and Barış Gökçe, "Design and Implementation of an Optimized PID Controller for Two-Limb Robot Arm Control," *Bitlis Eren Üniversitesi Fen Bilimleri Dergisi*, vol. 13, no. 1, pp. 192-204, https://doi.org/10.17798/bitlisfen.1370223.

[26] A. L. Shuraiji, and S. W. Shneen, "Fuzzy Logic Control and PID Controller for Brushless Permanent Magnetic Direct Current Motor: A Comparative Study," *Journal of Robotics and Control (JRC)*, vol. 3, no. 6, pp. 762-768, 2022, https://doi.org/10.18196/jrc.v3i6.15974.

[27] E. S. Rahayu, A. Ma'arif, and A. Cakan, "Particle swarm optimization (PSO) tuning of PID control on DC motor," *International Journal of Robotics and Control Systems*, vol. 2, no. 2, pp. 435-447, 2022, https://doi.org/10.31763/ijrcs.v2i2.476.

[28] M. G. Mohanan, and A. Salgaonkar, "Robotic motion planning in dynamic environments and its applications," *International Journal of Robotics and Control Systems*, vol. 2, vol. 4, pp. 666-691, 2022, https://doi.org/10.31763/ijrcs.v2i4.816.

[29] F. N. Abdullah, G. A. Aziz, and S. W. Shneen, "Simulation model of servo motor by using matlab," *Journal of Robotics and Control (JRC)*, vol. 3, no. 2, pp. 176-179, 2022, https://doi.org/10.18196/jrc.v3i2.13959.

[30] J. Możaryn, J. Petryszyn, and S. Ozana, "PLC based fractional-order PID temperature control in pipeline: design procedure and experimental evaluation," *Meccanica*, vol. 56, no. 4, pp. 855–871, 2021, https://doi.org/10.1007/s11012-020-01215-0.

[31] A. Setiawan and A. Ma'arif, "Stirring System Design for Automatic Coffee Maker Using OMRON PLC and PID Control," *International Journal of Robotics and Control Systems*, vol. 1, no. 3, pp. 390-401, 2021, https://doi.org/10.31763/ijrcs.v1i3.457.

[32] H. S. Dakheel, Z. B. Abdullah, N. S. Jasim, S. W. Shneen, "Simulation model of ANN and PID controller for direct current servo motor by using Matlab/Simulink," *TELKOMNIKA (Telecommunication Computing Electronics and Control)*, vol. 20, no. 4, pp. 922-932, 2022, http://doi.org/10.12928/telkomnika.v20i4.23248.

[33] G. Gabor and G. Livint, "Implementation of a PID Controller Using Siemens PLC," *2022 International Conference and Exposition on Electrical And Power Engineering (EPE)*, pp. 593-596, 2022, https://doi.org/10.1109/EPE56121.2022.9959869.

[34] K. Vanchinathan and N. Selvaganesan, "Adaptive fractional order PID controller tuning for brushless DC motor using Artificial Bee Colony algorithm," *Results in Control and Optimization*, vol. 4, p. 100032, 2021, https://doi.org/10.1016/j.rico.2021.100032.

[35] O. J. Tola, E. A. Umoh, E. A. Yahaya, "Pulse Width Modulation Analysis of Five-Level Inverter-Fed Permanent Magnet Synchronous Motors for Electric Vehicle Applications," *International Journal of Robotics and Control Systems*, vol. 1, no. 4, pp. 477-487, 2021, https://doi.org/10.31763/ijrcs.v1i4.483.

[36] M. A. Shamseldin, R. Barbosa, and I. Jesus, "Optimal Coronavirus Optimization Algorithm Based PID Controller for High Performance Brushless DC Motor," *Algorithms*, vol. 14, no. 7, p. 193, 2021, https://doi.org/10.3390/a14070193.

[37] G. R. Wicaksono and R. D. Puriyanto, "Programmable Logic Controller (PLC) Based Paint Viscosity Control System," *Buletin Ilmiah Sarjana Teknik Elektro*, vol. 3, no. 1, pp. 1-9, 2021, https://doi.org/10.12928/biste.v3i1.1109.

[38] M. Khalifa, A. H. Amhedb, and M. A. Sharqawi, "Position Control of Real Time DC Motor Using LabVIEW," *Journal of Robotics and Control (JRC)*, vol. 2, no. 5, pp. 342–348, 2021, https://doi.org/10.18196/jrc.25104.

[39] P. B. D. M. Oliveira, J. D. Hedengren, and E. J. S. Pires, "Swarm-Based Design of Proportional Integral and Derivative Controllers Using a Compromise Cost Function: An Arduino Temperature Laboratory Case Study," *Algorithms*, vol. 13, no. 12, p. 315, 2020, https://doi.org/10.3390/a13120315.

[40] A. Ma'arif, I. Cahyadi, S. Herdjunanto, and O. Wahyunggoro, "Tracking Control of High Order Input Reference Using Integrals State Feedback and Coefficient Diagram Method Tuning," *IEEE Access*, vol. 8, pp. 182731–182741, 2020, https://doi.org/10.1109/ACCESS.2020.3029115.

[41] B. N. Kommula and V. R. Kota, "Direct instantaneous torque control of Brushless DC motor using firefly Algorithm based fractional order PID controller," *Journal of King Saud University - Engineering Sciences*, vol. 32, no. 2, pp. 133–140, 2020, https://doi.org/10.1016/j.jksues.2018.04.007.

[42] E. W. Suseno, and A. Ma'arif, "Tuning of PID controller parameters with genetic algorithm method on DC motor," *International Journal of Robotics and Control Systems*, vo1. 1, no. 1, pp. 41-53, 2021, https://doi.org/10.31763/ijrcs.v1i1.249.

[43] M. F. A. Andzar and R. D. Puriyanto, "PID Control for Temperature and Motor Speed Based on PLC," *Signal and Image Processing Letters*, vol. 1, no. 1, pp. 7-13, 2019, https://doi.org/10.31763/simple.v1i1.150.

[44] S. W. Jeaeb, A. Z. Salman, Q. A. Jawad, H. Shareef, "Advanced optimal by PSO-PI for DC motor," *Indonesian Journal of Electrical Engineering and Computer Science*, vol. 16, no. 1, pp. 165-175, 2019, http://doi.org/10.11591/ijeecs.v16.i1.pp165-175.

[45] D. Potnuru, K. Alice Mary, and C. Sai Babu, "Experimental implementation of Flower Pollination Algorithm for speed controller of a BLDC motor," *Ain Shams Engineering Journal*, vol. 10, no. 2, pp. 287–295, 2019, https://doi.org/10.1016/j.asej.2018.07.005.

[46] B. Hekimoğlu, "Optimal Tuning of Fractional Order PID Controller for DC Motor Speed Control via Chaotic Atom Search Optimization Algorithm," *IEEE Access*, vol. 7, pp. 38100-38114, 2019, https://doi.org/10.1109/ACCESS.2019.2905961.

[47] S. Waley, C. Mao, and N. K. Bachache, "Biogeography based optimization for tuning FLC controller of PMSM," *Advances in Swarm and Computational Intelligence*, pp. 395-402, 2015, https://doi.org/10.1007/978-3-319-20466-6_42.

[48] M. S. Chehadeh and I. Boiko, "Design of rules for in-flight non-parametric tuning of PID controllers for unmanned aerial vehicles," *Journal of the Franklin Institute*, vol. 356, no. 1, pp. 474-491, 2019, https://doi.org/10.1016/j.jfranklin.2018.10.015.

[49] A. Maarif, A. I. Cahyadi, S. Herdjunanto, Iswanto, Y. Yamamoto, "Tracking Control of Higher Order Reference Signal Using Integrators and State Feedback," *IAENG International Journal of Computer Science*, vol. 46, no. 2, pp. 208-216, 2019, https://www.iaeng.org/IJCS/issues_v46/issue_2/IJCS_46_2_09.pdf.

[50] H. S. Dakheel, Z. B. Abdullah, and S. W. Shneen, "Simulation model of FLC-PID based speed control system for DC motor drive by using matlab," *AIP Conference Proceedings*, vol. 3002, no. 1, 2024, https://doi.org/10.1063/5.0206580.

[51] A. M. Zaki, M. El-Bardini, F. A. S. Soliman, and M. M. Sharaf, "Embedded two level direct adaptive fuzzy controller for DC motor speed control," *Ain Shams Engineering Journal*, vol. 9, no. 1, pp. 65–75, 2018, https://doi.org/10.1016/j.asej.2015.10.003.

[52] I. D. Kurniasari and A. Ma'arif, "Implementing PID-Kalman Algorithm to Reduce Noise in DC Motor Rotational Speed Control," *International Journal of Robotics and Control Systems*, vol. 4, no. 2, pp. 958-978, 2024, https://doi.org/10.31763/ijrcs.v4i2.1309.

[53] A. Ma'arif, A. I. Cahyadi, and O. Wahyunggoro, "CDM Based Servo State Feedback Controller with Feedback Linearization for Magnetic Levitation Ball System," *International Journal on Advanced Science, Engineering and Information Technology*, vol. 8, no. 3, pp. 930–937, 2018, https://doi.org/10.18517/ijaseit.8.3.1218.